JOURNAL OF BACTERIOLOGY, May 2011, p. 2341–2346 Vol. 193, No. 9
0021-9193/11/$12.00 doi:10.1128/JB.00074-11

Identification of *Streptococcus pneumoniae* Cps2C Residues That Affect Capsular Polysaccharide Polymerization, Cell Wall Ligation, and Cps2D Phosphorylation▽†

James P. Byrne, Judy K. Morona, James C. Paton,* and Renato Morona

Research Centre for Infectious Diseases, School of Molecular and Biomedical Science, University of Adelaide, Adelaide, S.A. 5005, Australia

Received 17 January 2011/Accepted 18 February 2011

A number of single amino acid substitutions throughout *Streptococcus pneumoniae* Cps2C were found to affect its function and confer either a mucoid or a small colony phenotype. These mutants exhibit significant changes in capsular polysaccharide (CPS) profile relative to that of wild-type pneumococci. The introduced mutations affect either polymerization or ligation of CPS to the cell wall and/or Cps2D phosphorylation.

Streptococcus pneumoniae (the pneumococcus) is an important cause of invasive disease in human populations throughout the world. One of the key virulence factors it possesses is its capsular polysaccharide (CPS), of which there are currently over 90 structurally distinct serotypes. In all serotypes, the CPS is essential for pneumococcal virulence due to its role in resistance to host phagocytic clearance mechanisms (1, 7, 9).

Despite the differences between the polysaccharide repeat unit structures, all but 2 serotypes (3 and 37) utilize similar biosynthetic machinery. The pneumococcal CPS biosynthesis (*cps*) loci contain four genes common to all of these serotypes, with the exception of serotypes 3 and 37, which use distinct biosynthetic and regulatory machinery (6). These common genes, *cpsA* to *cpsD*, are located at the 5′ end of the loci and have been implicated in the regulation of CPS biosynthesis (11).

CpsA is predicted to be a transcriptional activator, and colonies of *cpsA* deletion mutants appear significantly smaller and duller than those of the wild type (WT). The mutant colonies also show reduced signal intensity when probed by anticapsular antibodies and viewed by microscopy (11). CpsB is a manganese-dependent phosphotyrosine protein phosphatase belonging to the polymerase and histidinol phosphatase family. It is known to positively regulate CPS biosynthesis by dephosphorylating CpsD (11, 13). The membrane protein CpsC contains two short cytoplasmic regions at the amino and carboxy terminals, two transmembrane (TM) helices, and a series of alternating α-helices and β-strands within a large extracellular loop region of the protein (Fig. 1A) (14). Currently, no structural data exist for CpsC and no functional domains have been identified. The last component of the regulatory machinery is CpsD, an autophosphorylating protein-tyrosine kinase known to require interaction with CpsC to be functional (13, 16, 18). Both CpsC and CpsD belong to the polysaccharide copolymerase 2b (PCP2b) protein family, and the activity of CpsC and CpsD is analogous to that observed in the full-length PCP2a protein Wzc from *Escherichia coli* (15, 17, 19). Phosphorylation of CpsD has been shown to negatively regulate the biosynthesis of CPS (12, 13).

CpsB, CpsC, and CpsD are proposed to function together to generate a phosphorylation cycle across CpsD, similarly to the CapC-CapA-CapB system previously described in *Staphylococcus aureus* (5), and through this cycle, CPS polymer biosynthesis and ligation are predicted to be controlled.

Based on previous work by Morona et al. (16, 18) and the results of this study, we propose a greater role for CpsC in CPS biosynthesis, as mutagenesis of Cps2C results in the generation of multiple mutant colony morphologies classified as small, mucoid, or rough (12).

Construction of hemagglutinin (HA) epitope-tagged Cps2C mutants of *S. pneumoniae* D39. To facilitate the analysis of various D39 Cps2C mutants (listed in Table 1), we inserted the erythromycin resistance cassette *erm* between *cps2B* and *cps2C* and DNA encoding a dual HA tag (YPYDVPDYAAAYPYDVPDYA) at the 5′ end of *cps2C* in *S. pneumoniae* D39 (serotype 2), as shown in Fig. 2 (designated D39:EHA-Cps2C). A series of overlapping oligonucleotide primers in combination with flanking oligonucleotide primers located in *cps2B* and *cps2D* (see Table S1 in the supplemental material) were then used to introduce single amino acid codon changes throughout the HA-tagged *cps2C* gene using overlap extension PCR (OEPCR), a technique that has been previously described (8).

Characterization of defined Cps2C mutants. Following the transformation of D39 with the various OEPCR products, transformants were screened for Erm^r and the region spanning *cps2B*, the mutated *HA-cps2C*, and *cps2D* was subjected to DNA sequencing to confirm correct mutation (data not shown).

CPS expression by the mutants was first determined by quellung reaction using typing serum obtained from Statens Seruminstitut (Copenhagen, Denmark). Mutants positive for CPS were assessed for colony phenotype as WT, mucoid, or small as previously described by Morona et al. (12); those negative for

* Corresponding author. Mailing address: School of Molecular and Biomedical Science, University of Adelaide, Adelaide, S.A. 5005, Australia. Phone: 61-8-83035929. Fax: 61-8-83033262. E-mail: james.paton@adelaide.edu.au.

† Supplemental material for this article may be found at http://jb.asm.org/.

▽ Published ahead of print on 4 March 2011.

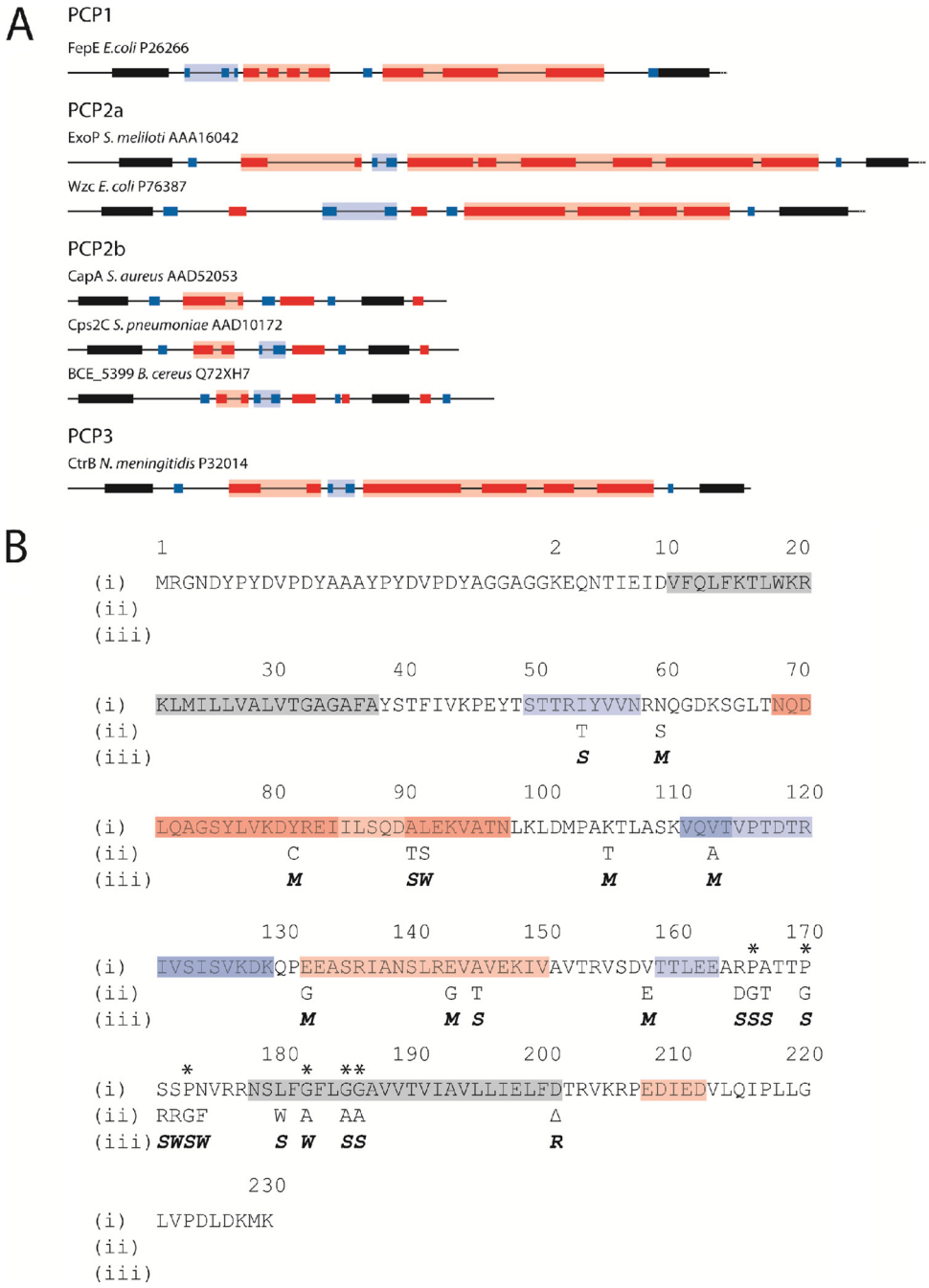

FIG. 1. Predicted secondary structures of selected PCP2 proteins. (A) Complete open reading frames of selected PCP2 proteins were submitted to the Predict Protein server (http://www.predictprotein.org/), and the outputs from the programs PHDhtm (Predict transmembrane) and PROF (Predict secondary structure) were used to predict TM regions and secondary-structure features, respectively. Only the periplasmic region between TM1 and TM2 (solid black shading) are shown. Red shading denotes α-helix; blue shading denotes β-strand; intense color shading represents high-scoring regions (PROF score, 7 to 9); faint color shading represents low-scoring regions (PROF score, 4 to 6). (B) Amino acid sequences of D39:EHA-Cps2C and site-directed mutants. (i) Amino acid sequence of D39:EHA-Cps2C with predicted secondary structure (http://www.predictprotein.org/) superimposed: gray, TM helix; red, α-helix; blue, β-strand. Amino acid numbering ignores the dual HA tag insert to facilitate comparison to the D39:Cps2C sequence. Asterisks indicate highly conserved proline and glycine residues preceding and within TM2. (ii) Amino acid substitutions are indicated. (iii) Phenotypic change resulting from amino acid sequence changes: M, mucoid phenotype; S, small colony phenotype; W, WT; R, rough phenotype.

CPS were classified as rough. The results of the colony phenotype determination are shown in Table 1.

All of the mucoid mutants had amino acid substitutions located in the extracellular loop of Cps2C but were not predicted to greatly alter the secondary structure of Cps2C (Fig. 1B) on the basis of computer modeling using the Predict Protein server (http://www.predictprotein.org/). N60S, K106T, and V159E all fall outside predicted secondary

TABLE 1. Strains used and constructed in this study

Strain	Colony phenotype	Description	Reference
D39	WT	*S. pneumoniae* serotype 2	
D39:BCDΔ	Rough	*cpsB*, *cpsC*, and *cpsD* genes replaced with *erm* in D39, Erm^r	12
D39:EHA-Cps2C	WT	*erm* inserted between *cpsB* and HA tagged *cpsC*, Erm^r	This study
D39:EHA-I54T	Small	Ile→Thr substitution at residue 54 (note that all mutants were constructed in the D39:EHA-Cps2C background)	This study
D39:EHA-N60S	Mucoid	Asn→Ser substitution at residue 60	This study
D39:EHA-Y82C	Mucoid	Tyr→Cys substitution at residue 82	This study
D39:EHA-A91T	Small	Ala→Thr substitution at residue 91	This study
D39:EHA-L92S	WT	Leu→Ser substitution at residue 92	This study
D39:EHA-K106T	Mucoid	Lys→Thr substitution at residue 106	This study
D39:EHA-V114A	Mucoid	Val→Ala substitution at residue 114	This study
D39:EHA-E133G	Mucoid	Glu→Gly substitution at residue 133	This study
D39:EHA-E144G	Mucoid	Glu→Gly substitution at residue 144	This study
D39:EHA-A146T	Small	Ala→Thr substitution at residue 146	This study
D39:EHA-V159E	Mucoid	Val→Glu substitution at residue 159	This study
D39:EHA-R166D	Small	Arg→Asp substitution at residue 166	This study
D39:EHA-P167G	Small	Pro→Gly substitution at residue 167	This study
D39:EHA-A168T	Small	Ala→Thr substitution at residue 168	This study
D39:EHA-P171G	Small	Pro→Gly substitution at residue 171	This study
D39:EHA-S172R	Small	Ser→Arg substitution at residue 172	This study
D39:EHA-S173R	WT	Ser→Arg substitution at residue 173	This study
D39:EHA-P174G	Small	Pro→Gly substitution at residue 174	This study
D39:EHA-N175F	WT	Asn→Phe substitution at residue 175	This study
D39:EHA-L181W	Small	Leu→Trp substitution at residue 181	This study
D39:EHA-G183A	WT	Gly→Ala substitution at residue 183	This study
D39:EHA-G186A	Small	Gly→Ala substitution at residue 186	This study
D39:EHA-G187A	Small	Gly→Ala substitution at residue 187	This study
D39:EHA-D202Δ	Rough	HA-*cps2C* truncated after residue 202	This study

structures, while Y82C, E133G, and E144G fall within α-helices and V114A lies within the second β-strand domain. However, none of these substitutions were predicted to alter the domains they reside in.

Amino acid substitutions resulting in small colony mutants predominantly localized to the proline- and glycine-rich domains preceding and within TM2 (Fig. 1B). It has previously been suggested that these highly conserved regions may be important for normal CPS biosynthesis and the function of Cps2C and related proteins (2, 4, 5). Apart from the proline residues themselves, we found that mutating some of the amino acids adjacent to the proline residues (R166D, A168T, and S172R) also resulted in the small colony phenotype.

The small colony phenotype-producing mutations that did not map to the proline- and glycine-rich region preceding and within TM2 are all present in secondary-structure domains in the extracellular loop. I54T is located in the first β-strand, while A91T and A146T are located in the first and second α-helices, respectively. Although these substitutions are located in regions of predicted secondary structure, they were not predicted to interfere with folding. However, the impact these mutations have on Cps2C's tertiary structure and function cannot yet be determined.

Western immunoblot analysis was performed to analyze Cps protein expression levels using (i) anti-HA (Sigma catalog no. H3663-200UL) to detect HA-tagged Cps2C, (ii) anti-Cps2D (13), and (iii) anti-phosphotyrosine (Santa Cruz Biotechnology catalog no. sc-7020) to detect the phosphorylated form of Cps2D (Cps2D~P). Lysates were obtained by growing cultures to an optical density at 600 nm (OD_{600}) of 0.6 in 20 ml of Todd-Hewitt broth with 0.5% yeast extract before resuspending the pellet in 400 μl of 2× Laemmli sample buffer (10). Lysates were separated on 4 to 12% Bis-Tris gradient gels (Invitrogen NuPAGE gel system; Invitrogen) before electrophoretic transfer onto nitrocellulose for HA-Cps2C and Cps2D detection and onto polyvinylidene fluoride membranes (Immobilon-P; Millipore) for Cps2D~P detection. After reaction with the appropriate antibody, labeling was detected using anti-mouse immunoglobulin G conjugated to horseradish peroxidase (KPL catalog no. 0748106) and Chemiluminescent Peroxidase Substrate-3 (Sigma catalog no. CPS3160-1KT) and visualized using a Kodak Image Station 4000MM Pro (Kodak).

Protein expression in all mutants was compared to that in D39 and D39:EHA-Cps2C to determine any deviation from WT protein expression levels (Fig. 3). The quantities of Cps2C and Cps2D appeared similar across all mutants, with the exception of D39:EHA-Cps2C:D202Δ, which shows an apparent reduction in the size of Cps2C (consistent with deletion of the 28 C-terminal amino acids) and a reduction in expression compared to that by D39:EHA-Cps2C.

The levels of Cps2D~P did not directly correlate with the small versus mucoid colony phenotype (as listed in Table 1) (Fig. 3). However, three of the small colony mutants, i.e., the P167G, A168T, and P171G mutants, had undetectable Cps2D~P and the R166D mutant (also small colony phenotype) expressed reduced levels. Clearly, residues 166 to 171 of Cps2C play a critical role in interaction with and transphosphorylation of Cps2D. Interestingly, P171 is one of the most highly conserved P residues in the PCP family, and this underscores the importance of Cps2C homologues in phosphorylative cycling.

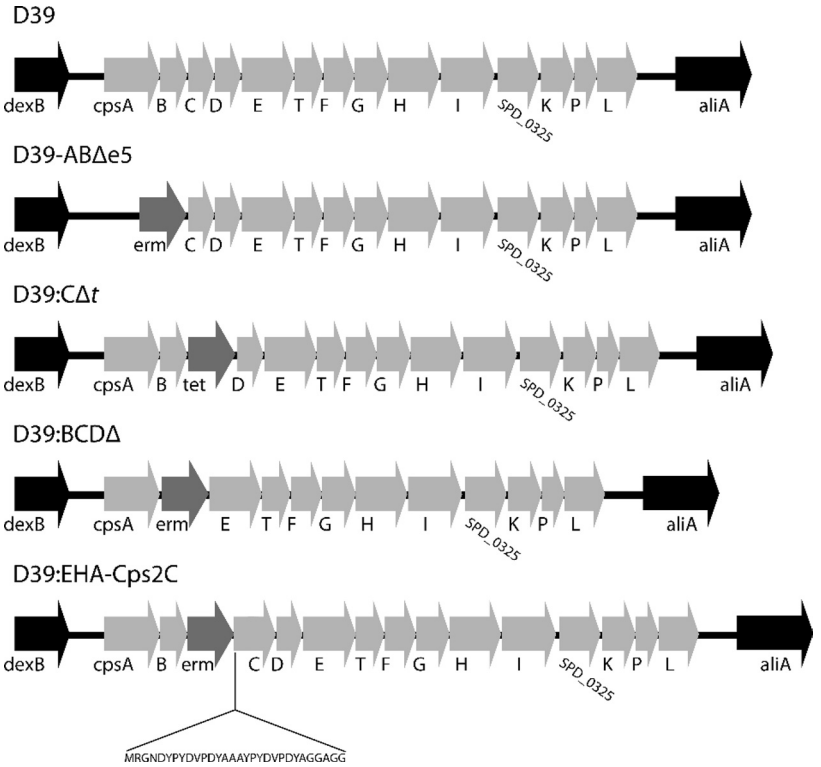

FIG. 2. Organization of the *cps* loci of strains used in this study. D39 was the parental strain for all work performed; gene nomenclature is as described for the sequence with GenBank accession no. YP_815832.1. D39:BCDΔ lacks *cps2B*, *cps2C*, and *cps2D*, as previously described (12). D39:EHA-Cps2C has *erm* inserted between *cps2B* and *cps2C* and the insertion of DNA encoding a small amino acid spacer sequence (RGND), the dual HA tag (YPYDVPDYAAAYPYDVPDYA), and a linker region (GGAGG) between the initiating Met1 and Lys2 of Cps2C.

Quantitation of CPS production by Cps2C mutants. The total CPS (T-CPS) and cell wall-associated CPS (CW-CPS) produced by each mutant were then compared to those produced by D39 and D39:EHA-Cps2C by using the colorimetric uronic acid assay (3), as glucuronic acid is a component of the type 2 CPS repeat unit. CPS levels were then expressed as a percentage of T-CPS production by WT D39 (Fig. 4; see Table S2 in the supplemental material for raw data).

It has previously been reported that D39 attaches ~55% of the CPS it produces to the cell wall (12), and this is also

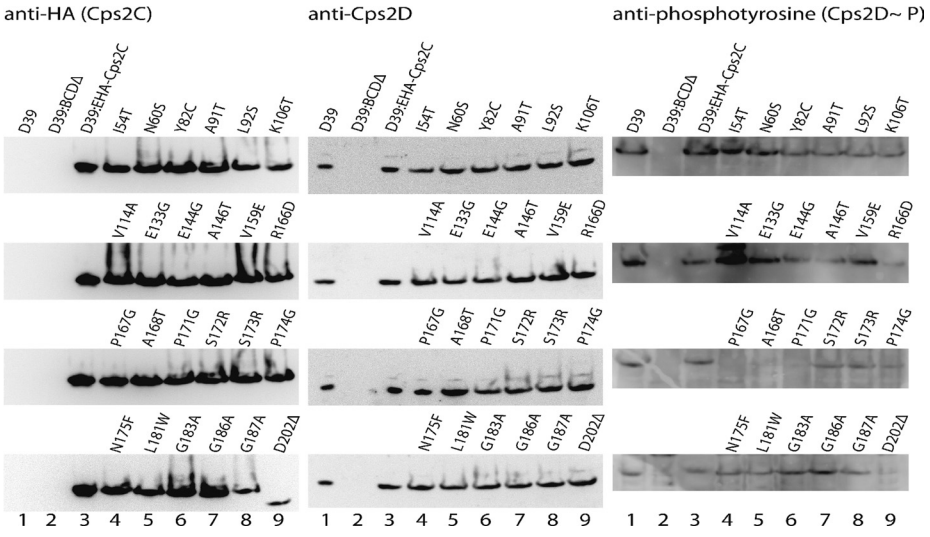

FIG. 3. Western blot analysis. Proteins in lysates from D39, D39:BCDΔ, D39:EHA-Cps2C, and the various mutants constructed as part of this study were separated by sodium dodecyl sulfate-polyacrylamide gel electrophoresis and analyzed by immunoblotting using anti-HA (to detect HA-Cps2C), anti-CpsD, or anti-phosphotyrosine (to detect Cps2D~P).

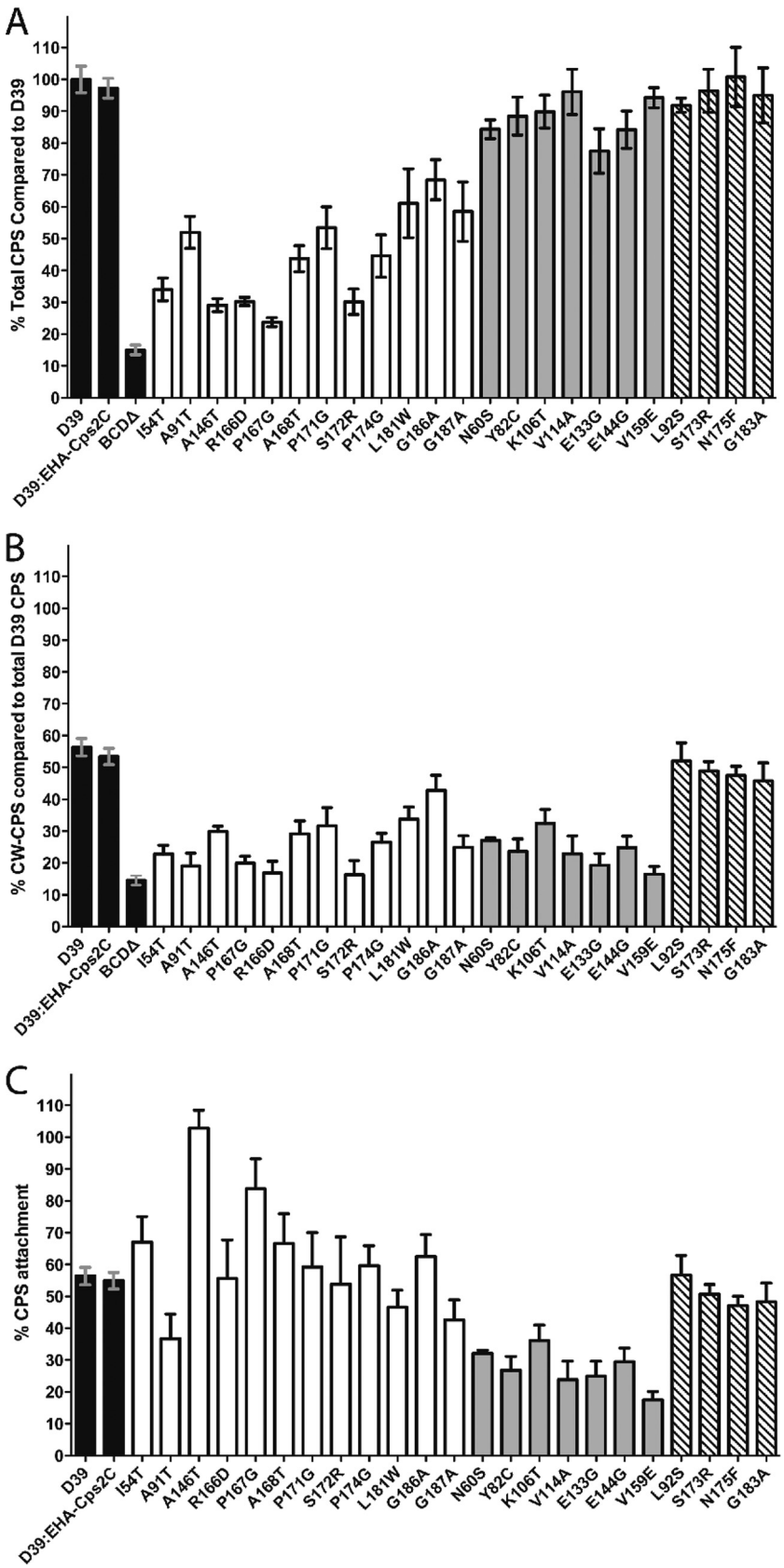

FIG. 4. Quantitation of CPS by uronic acid assay. (A) T-CPS produced by various mutants as a percentage of D39. (B) CW-CPS produced by the various mutants as a percentage of T-CPS for D39. (C) CW-CPS as a percentage of the T-CPS produced by each mutant. Shading indicates the colony phenotype as follows: black, control strain; white, small; gray, mucoid; striped, WT.

apparent from Fig. 4B and C. The WT Cps2C construct D39:EHA-Cps2C also produced and attached CPS at levels similar to those of D39, confirming that the HA-tagged Cps2C protein has WT activity (Fig. 4). All mucoid mutants had levels of T-CPS expression similar to those of the WT, while the small colony mutants produced significantly less T-CPS ($P < 0.0001$) (Fig. 4A). This supports the hypothesis that the small colony phenotype results from reduced CPS polymerization and may indicate lowered CPS polymerase (Cps2I) activity (12). The T-CPS levels of mucoid mutants were, as predicted, similar to WT T-CPS levels, suggesting no alteration to the CPS polymerase activity in these mutants.

CW-CPS levels detected for the small and mucoid colony types were both significantly lower than WT CW-CPS levels ($P < 0.0001$) (Fig. 4B), suggesting that the presence of mutated Cps2C induces a global downregulation of the CPS ligation machinery.

The percentage of CW-CPS compared to T-CPS for each mutant (defined here as the attachment percentage) was calculated to determine if any absolute changes in CPS attachment caused by Cps2C mutations can be observed (Fig. 4C). Small colony mutants show high proportions of attachment compared to those of all other groups. We suggest that as the small colony mutants have very low T-CPS, the amount of CW-CPS constitutes a greater proportion of the total CPS produced, resulting in elevated attachment percentages. To account for the increased percentage of CPS attachment, we suggest that there may be a finite number of available CPS attachment sites on the surface of the pneumococcus rather than an increase in the efficiency of the ligation machinery. In an environment with less T-CPS, as seen in the small colony mutants, saturation of sites available for CPS attachment would appear as a CPS attachment level higher than that of D39.

The mucoid mutants were found to have significantly lower attachment percentages ($P < 0.0001$) (Fig. 4C), with some mutants, such as the V159E mutant, having attachment percentages as low as 17.5% of the T-CPS they produce. This further supports the hypothesis that the mucoid colony phenotype is due to reduced ligation activity and not increased production of CPS. However, the actual mechanism of CPS ligation in *S. pneumoniae* has not yet been elucidated.

The only transformant not subjected to uronic acid assay was the truncation mutant D39:EHA-Cps2C:D202Δ. The assay was not performed as this mutant was observed to produce no detectable CPS by quellung reaction and so was classified as a rough mutant. To date, only gene deletion mutants have resulted in complete loss of CPS biosynthesis in *S. pneumoniae*, indicating that this C-terminal cytoplasmic region is critical for Cps2C function. This region probably plays a role in CPS biosynthesis and regulation similar to that of the cytoplasmic tail in *S. aureus* CapA (16, 18).

Further experiments aimed at narrowing down the regions of Cps2C involved in its activity and its interaction with Cps2D will facilitate a better understanding of the activities of these proteins and the regulation of CPS biosynthesis in *S. pneumoniae*.

This work was supported by program grant 565526 from the National Health and Medical Research Council of Australia (NHMRC). J.C.P. is an NHMRC Australia Fellow.

REFERENCES

1. **Austrian, R.** 1981. Pneumococcus: the first one hundred years. Rev. Infect. Dis. **3:**183–189.
2. **Becker, A., and A. Puhler.** 1998. Specific amino acid substitutions in the proline-rich motif of the *Rhizobium meliloti* ExoP protein result in enhanced production of low-molecular-weight succinoglycan at the expense of high-molecular-weight succinoglycan. J. Bacteriol. **180:**395–399.
3. **Blumenkrantz, N., and G. Asboe-Hansen.** 1973. New method for quantitative determination of uronic acids. Anal. Biochem. **54:**484–489.
4. **Dams-Kozlowska, H., and D. L. Kaplan.** 2007. Protein engineering of *wzc* to generate new emulsan analogs. Appl. Environ. Microbiol. **73:**4020–4028.
5. **Daniels, C., and R. Morona.** 1999. Analysis of *Shigella flexneri* Wzz (Rol) function by mutagenesis and cross-linking: Wzz is able to oligomerize. Mol. Microbiol. **34:**181–194.
6. **Dillard, J. P., and J. Yother.** 1994. Genetic and molecular characterization of capsular polysaccharide biosynthesis in *Streptococcus pneumoniae* type 3. Mol. Microbiol. **12:**959–972.
7. **Henrichsen, J.** 1995. Six newly recognized types of *Streptococcus pneumoniae*. J. Clin. Microbiol. **33:**2759–2762.
8. **Horton, R. M.** 1993. In vitro recombination and mutagenesis of DNA: SOEing together tailor-made genes, p. 251–261. *In* B. A. White (ed.), PCR protocols: current methods and applications. Humana Press Inc., Totowa, NJ.
9. **Kadioglu, A., J. N. Weiser, J. C. Paton, and P. W. Andrew.** 2008. The role of *Streptococcus pneumoniae* virulence factors in host respiratory colonization and disease. Nat. Rev. Microbiol. **6:**288–301.
10. **Laemmli, U. K.** 1970. Cleavage of structural proteins during the assembly of the head of bacteriophage T4. Nature **227:**680–685.
11. **Morona, J. K., D. C. Miller, R. Morona, and J. C. Paton.** 2004. The effect that mutations in the conserved capsular polysaccharide biosynthesis genes *cpsA*, *cpsB*, and *cpsD* have on virulence of *Streptococcus pneumoniae*. J. Infect. Dis. **189:**1905–1913.
12. **Morona, J. K., R. Morona, and J. C. Paton.** 2006. Attachment of capsular polysaccharide to the cell wall of *Streptococcus pneumoniae* type 2 is required for invasive disease. Proc. Natl. Acad. Sci. U. S. A. **103:**8505–8510.
13. **Morona, J. K., J. C. Paton, D. C. Miller, and R. Morona.** 2000. Tyrosine phosphorylation of CpsD negatively regulates capsular polysaccharide biosynthesis in *Streptococcus pneumoniae*. Mol. Microbiol. **35:**1431–1442.
14. **Morona, R., L. Purins, A. Tocilj, A. Matte, and M. Cygler.** 2009. Sequence-structure relationships in polysaccharide co-polymerase (PCP) proteins. Trends Biochem. Sci. **34:**78–84.
15. **Morona, R., L. Van Den Bosch, and C. Daniels.** 2000. Evaluation of Wzz/MPA1/MPA2 proteins based on the presence of coiled-coil regions. Microbiology **146**(Pt. 1)**:**1–4.
16. **Olivares-Illana, V., et al.** 2008. Structural basis for the regulation mechanism of the tyrosine kinase CapB from *Staphylococcus aureus*. PLoS Biol. **6:**e143.
17. **Paiment, A., J. Hocking, and C. Whitfield.** 2002. Impact of phosphorylation of specific residues in the tyrosine autokinase, Wzc, on its activity in assembly of group 1 capsules in *Escherichia coli*. J. Bacteriol. **184:**6437–6447.
18. **Soulat, D., et al.** 2006. *Staphylococcus aureus* operates protein-tyrosine phosphorylation through a specific mechanism. J. Biol. Chem. **281:**14048–14056.
19. **Vincent, C., et al.** 1999. Cells of *Escherichia coli* contain a protein-tyrosine kinase, Wzc, and a phosphotyrosine-protein phosphatase, Wzb. J. Bacteriol. **181:**3472–3477.